

Direct validation of radiosonde data against radio occultation bending angles

A. von Engel'n & RO Team@EUMETSAT

GRUAN/ICM-14, Nov/Dec 2022





Radio Occultation (RO) Overview/Motivation

Bending Angles from RO/Sondes

Comparing AWI & Lindenberg / GRUAN to GRAS

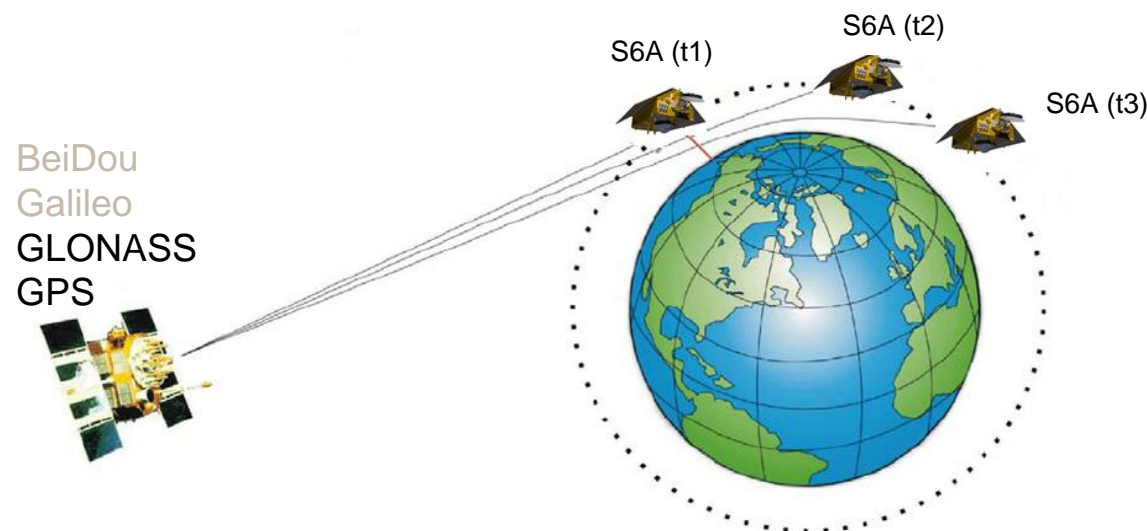
Conclusion / Future Work

RO Overview



Observe GNSS signals (e.g. GPS, GLONASS):

- through atmosphere limb in rising, setting
- zenith direction for Precise LEO Orbit/Clock
- about 500–600 occultations/day/GNSS
- neutral atmospheric occultations:
 - ground to about 60km, <1km vertical resolution
 - weather independent, very stable (time based)
- **Typical Products:**
 - bending angle at level 1b
 - refractivity at level 2
 - temperature, water vapour at level 2
 - gridded data at level 3
- **Typical applications:**
 - weather forecasting
 - climate, re-analysis
- **S6 Services:**
 - Near Real Time (NASA/JPL), level 1b, 2 within 3h, operational since August 2021
 - Non Time Critical (EUMETSAT/ROM SAF), level 1b, 2, 3 within about 3 weeks, operational since November 2021



Radio Occultation Principle: Observation of e.g. GPS or GLONASS satellite signals through the atmosphere; changing refractivity leads to bending of rays. The GNSS-RO instrument on S6A is built by JPL/NASA and observes both, GPS and GLONASS.



- Validation of RO vs. radio sondes generally done by processing RO data to temperature and water vapour, involving several processing steps and use of a priori information (or, use refractivity which smoothes the data)
- Generating bending angles from radio sonde data would not involve a priori data, and allows to validate directly on the RO FCDR, with the original high resolution
- In particular interesting in the lower troposphere, where separating temperature and water vapour information requires a priori, and where RO has biases due to super refraction, low SNR, etc

2.2 Atmospheric Bending and Refractive Index Profile Retrieval: Theory

2.2.1 Atmospheric refraction and spherical symmetry. In the geometric optics approximation to the propagation of electromagnetic radiation the path of a ray passing through a region of varying refractive index is determined globally by Fermat's principle of least time and locally by Snell's law. In the most general case, it is not possible to retrieve the three-dimensional variation of index of refraction n from measurements of α as a function of a during an occultation. However, the variation of n along a limb path in the Earth's atmosphere is dominated by the vertical density gradient so that, to the first order, the gradient of n is directed radially and the local refractive index field is spherically symmetrical such that the total refractive bending angle is

$$\alpha(a) = 2 \int_{r_t}^{\infty} d\alpha = 2a \int_{r_t}^{\infty} \frac{1}{\sqrt{r^2 n^2 - a^2}} \frac{d \ln(n)}{dr} dr \quad (1)$$

where r is distance from the center of curvature and the integral is over the portion of the atmosphere above r_t . Equation (1), the forward calculation of $\alpha(a)$ given $n(r)$, can be inverted by using an Abelian transformation to express $n(r)$ in terms of α and a [Fjeldbo *et al.*, 1971].

$$n(r) = \text{Exp} \left[\frac{1}{\pi} \int_{a_1}^{\infty} \frac{\alpha}{\sqrt{a^2 - a_1^2}} da \right] \quad (2)$$

where $a_1 = nr$ is the impact parameter for the ray whose tangent radius is r . Given $\alpha(a)$, (2) can be evaluated numerically.

2.3.1. The dependence of refractive index on atmospheric properties. In order to derive atmospheric properties from retrieved profiles of the real component of atmospheric refractive index n , it is necessary to know how these properties influence n . At microwave wavelengths in the Earth's atmosphere, n contains contributions from four main sources. These are, in order of importance, the dry neutral atmosphere, water vapor, free electrons in the ionosphere, and particulates (primarily liquid water). Their effects are given to first order by

$$N = (n-1) \times 10^6 = 77.6 \frac{P}{T} + 3.73 \times 10^5 \frac{P_w}{T^2} + 4.03 \times 10^7 \frac{n_e}{f^2} + 1.4 W \quad (7)$$

where N is refractivity, P is atmospheric pressure in mbar, T is atmospheric temperature in Kelvin, P_w is water vapor partial pressure in mbar, n_e is electron number density per cubic meter, f is transmitter frequency in Hertz, and W is liquid water content in grams per cubic meter. Throughout this paper, the

JOURNAL OF GEOPHYSICAL RESEARCH, VOL. 102, NO. D19, PAGES 23,429–23,465, OCTOBER 20, 1997

Observing Earth's atmosphere with radio occultation measurements using the Global Positioning System

E. R. Kursinski¹

Division of Geological and Planetary Sciences, California Institute of Technology, Pasadena

G. A. Hajj, J. T. Schofield, and R. P. Linfield

Jet Propulsion Laboratory, California Institute of Technology, Pasadena

K. R. Hardy

AS&T, Palo Alto, California

Bending Angles from RO/Sondes





- Using either AWI Polarstern¹ (from 2000 onwards) or GRUAN² (v2) radio sondes
- Using Metop-A, -B reprocessed data (v2.0, few years old)
- Using ERA5 collocated to radio sonde
- Collocations within 3h and 300km
- Using a simplified bending angle forward operator:
 - compared to reference ROPP one, and has only minor differences
 - as ROPP, integrates upwards with an exponential refractivity

¹ <https://doi.org/10.1594/PANGAEA.882736>

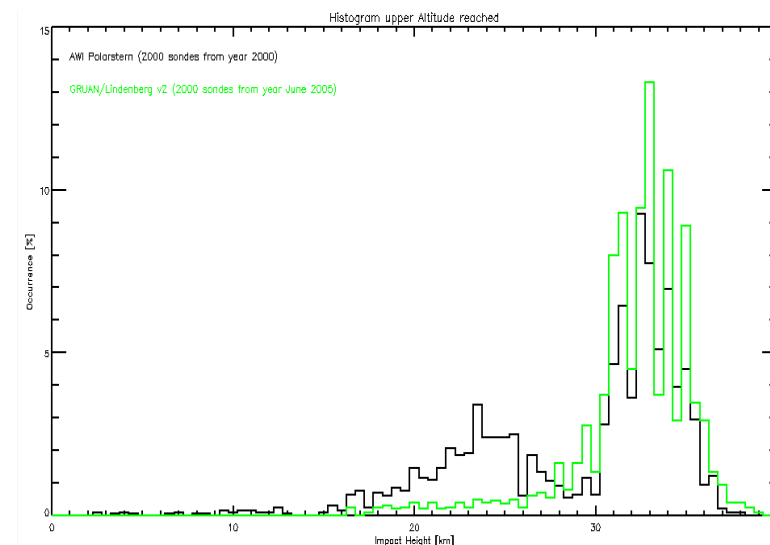
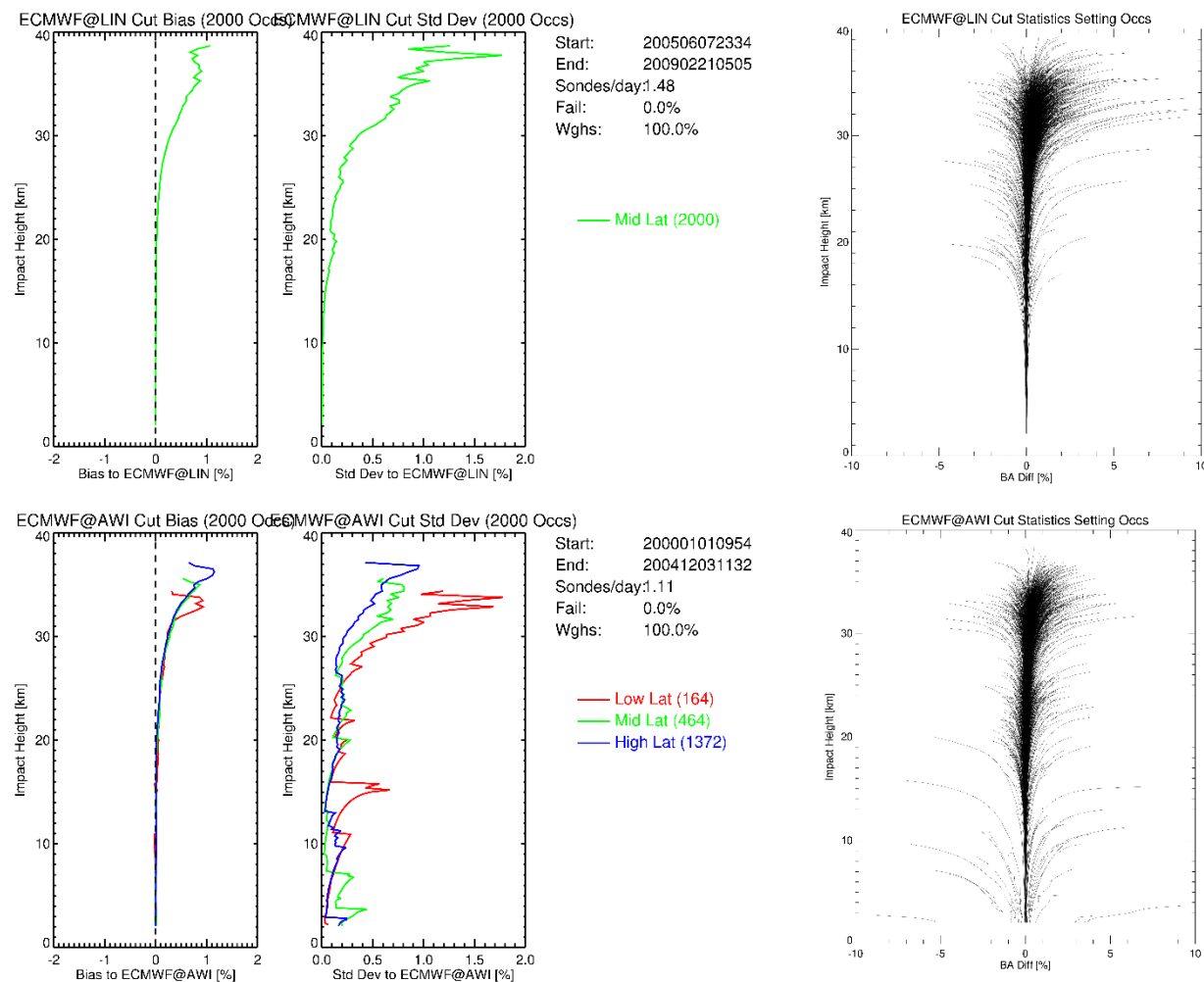
² [10.5676/GRUAN/RS92-GDP.2](https://doi.org/10.5676/GRUAN/RS92-GDP.2)

Note: Radio sondes are unassigned, can be represented as setting or rising occultations

Initial Tests with AWI/Lindenberg

www.eumetsat.int

Just use first 2000 sonde time/location/vertical coverage within ERA5, and assess the impact of the missing atmosphere above sonde.



Histogram of the first 2000 AWI and GRUAN/Lindenberg highest altitude reached

Bias (left) standard deviation (middle), spaghetti plot (right) of AWI (bottom) and GRUAN/Lindenberg (top) for first 2000 sonde times locations, comparing bending angles using full ECMWF at sonde location, or cut to maximum sonde altitude.

Comparing AWI & Lindenberg & GRUAN to GRAS

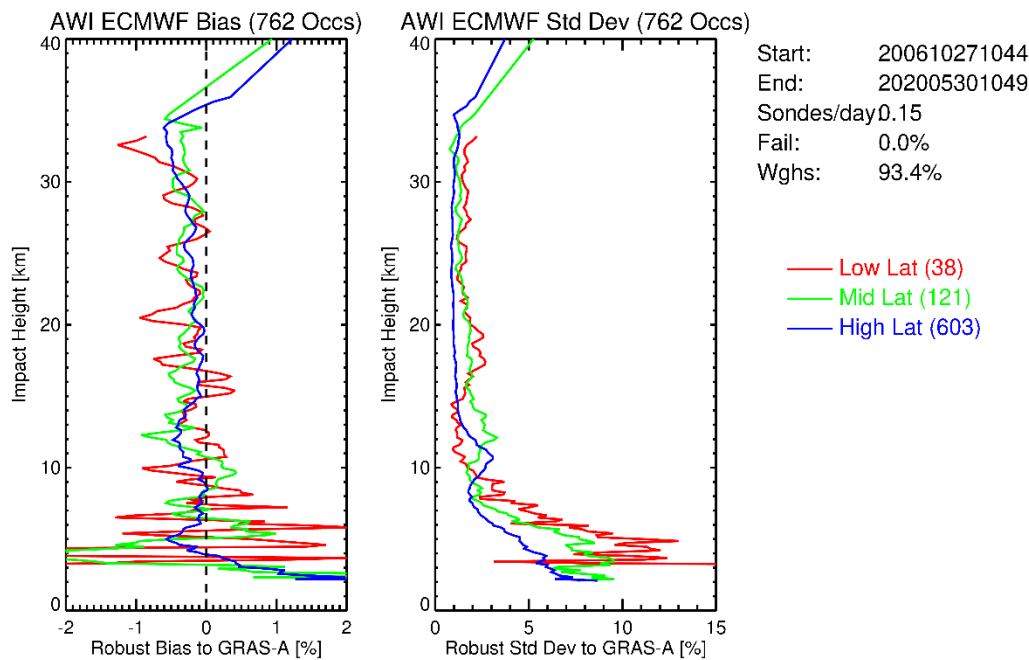
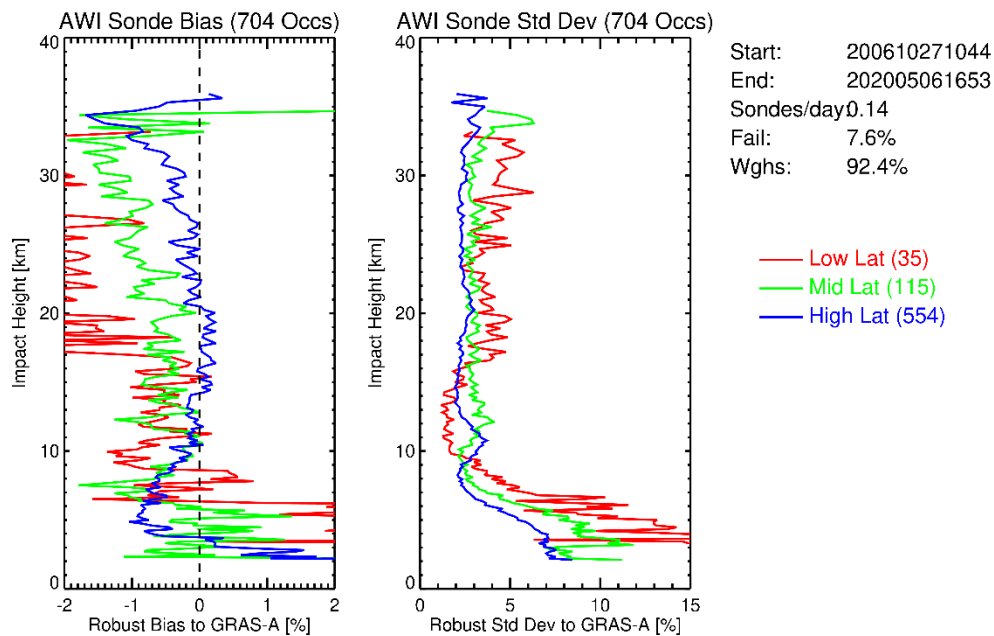




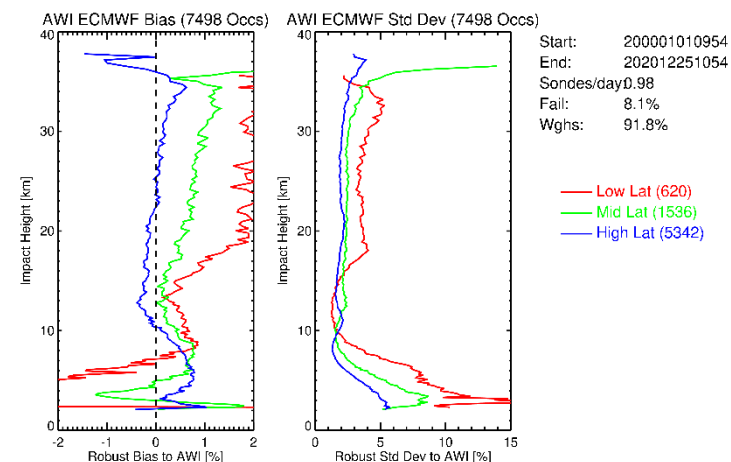
Comparing to GRAS Metop-A

www.eumetsat.int

Collocate Metop-A/GRAS 300km/3h against AWI Polarstern



Bias and standard deviation of AWI Polarstern match against Metop-A (top left), ECMWF at AWI against Metop-A (top right), and ECMWF at AWI against AWI (bottom right). Legend provides coverage, average sondes/day, RO/match failures, outliers/weight.

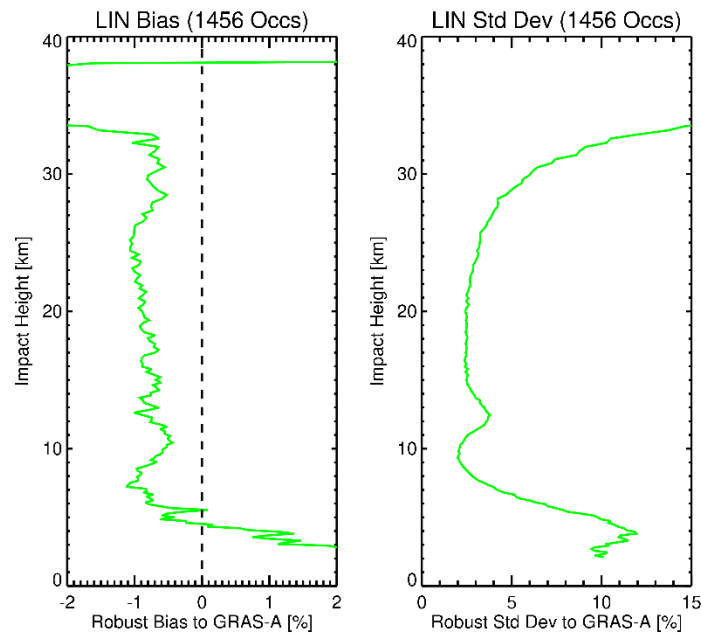




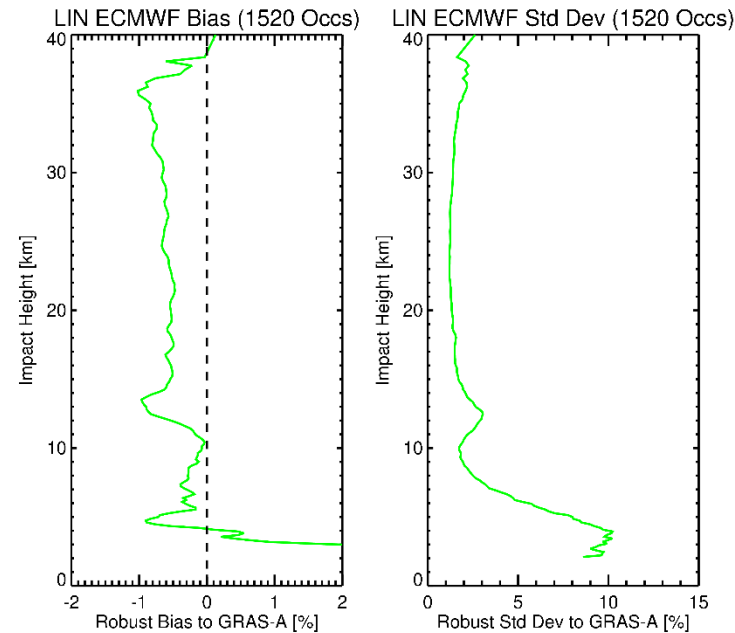
Comparing to GRAS Metop-A

www.eumetsat.int

Collocate Metop-A/GRAS 300km/3h against GRUAN/Lindenberg

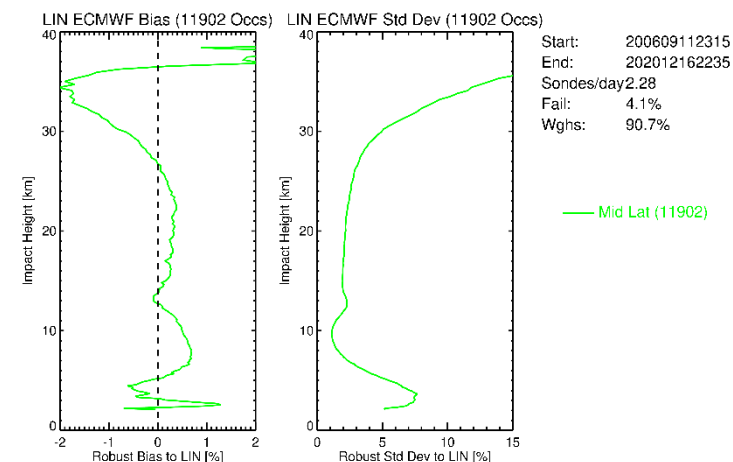


— Mid Lat (1456)



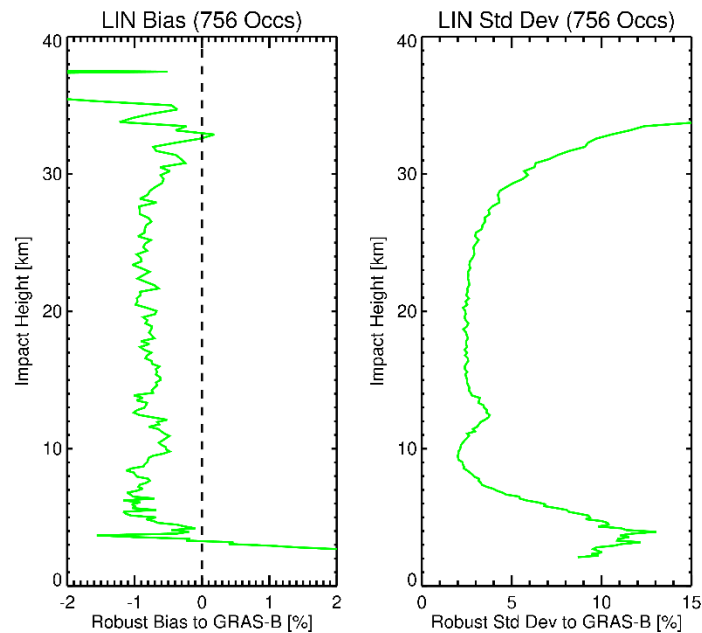
— Mid Lat (1520)

Bias and standard deviation of Lindenberg match against Metop-A (top left), ECMWF at Lindenberg against Metop-A (top right), and ECMWF at Lindenberg against Lindenberg (bottom right). Legend provides coverage, average sondes/day, RO/match failures, outliers/weight.

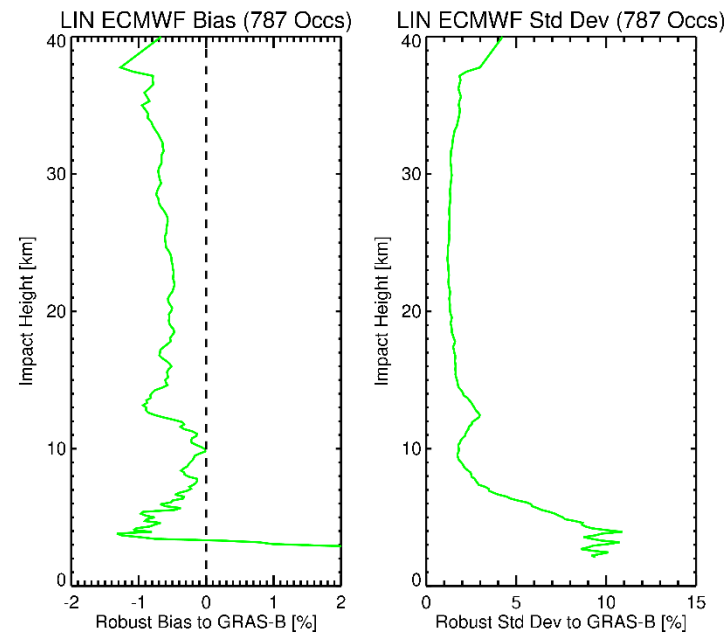


— Mid Lat (11902)

Collocate Metop-B/GRAS 300km/3h against GRUAN/Lindenberg



Start: 201210021045
 End: 201907102255
 Sondes/day 0.31
 Fail: 3.9%
 Wghs: 92.9%



Start: 201210021045
 End: 201907102255
 Sondes/day 0.32
 Fail: 0.0%
 Wghs: 93.7%

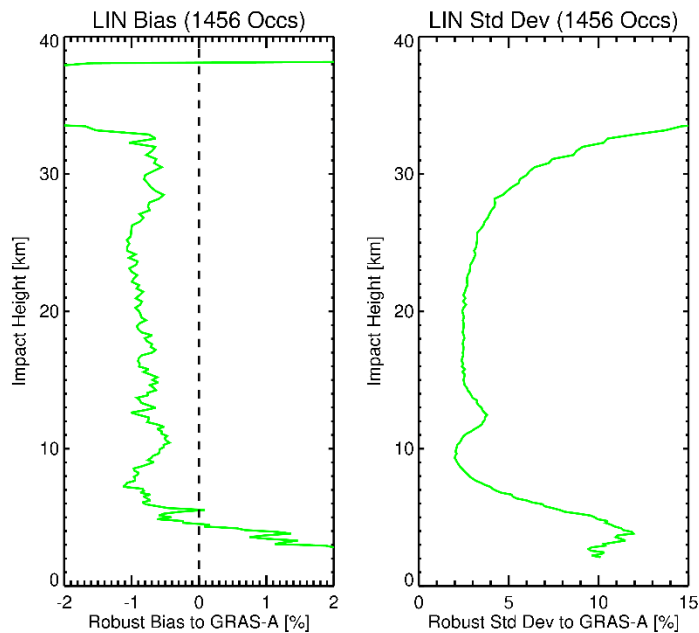
Bias and standard deviation of Lindenberg match against Metop-B (left), ECMWF at Lindenberg against Metop-B (right). Legend provides coverage, average sondes/day, RO/match failures, outliers/weight.



Comparing to LIN Red. Accuracy to GRAS Metop-A

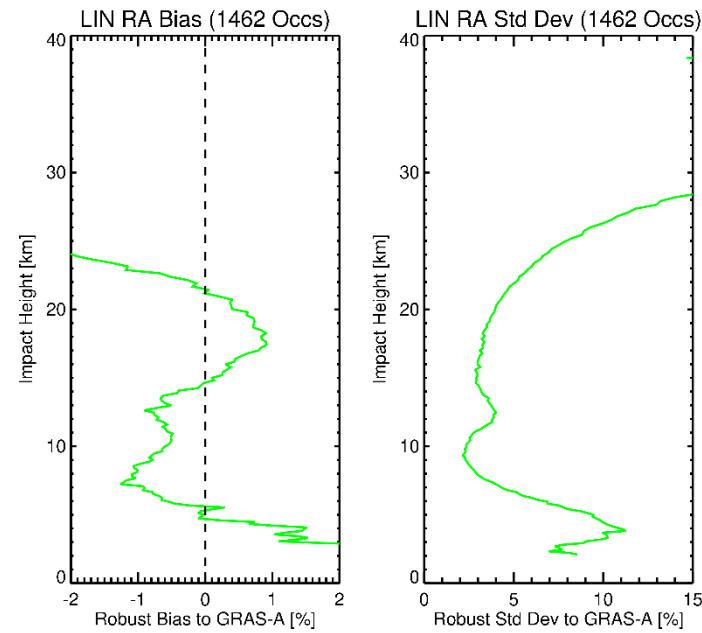
www.eumetsat.int

Collocate Metop-A/GRAS 300km/3h against GRUAN/Lindenberg, reduce accuracy to F0.1, RH 1% high up



Start: 200706051820
End: 202002191732
Sondes/day 0.31
Fail: 4.2%
Wghs: 92.8%

— Mid Lat (1456)



Start: 200706051820
End: 202002191732
Sondes/day 0.31
Fail: 3.8%
Wghs: 93.6%

— Mid Lat (1462)

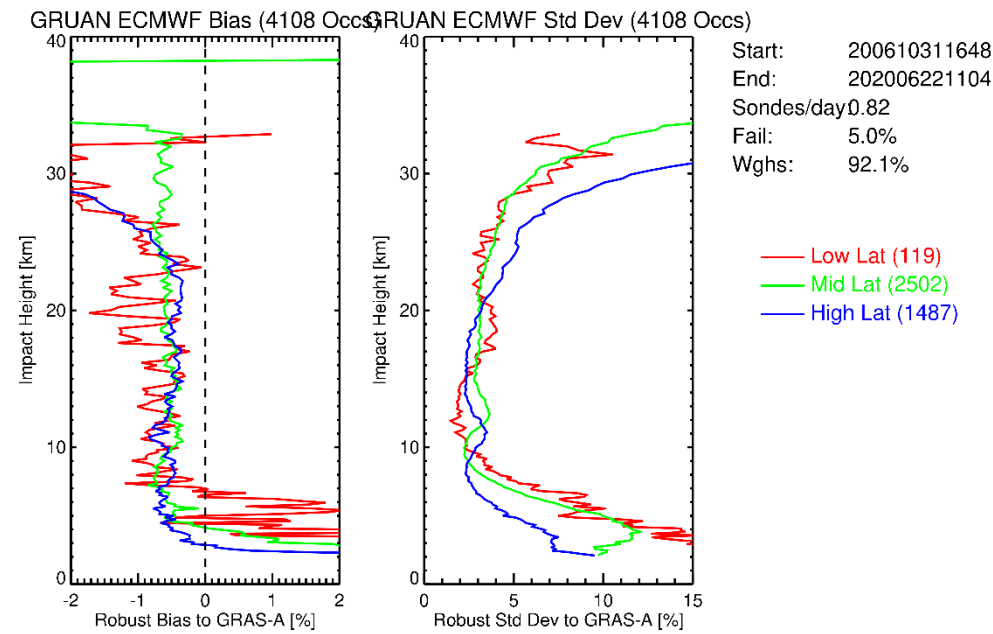
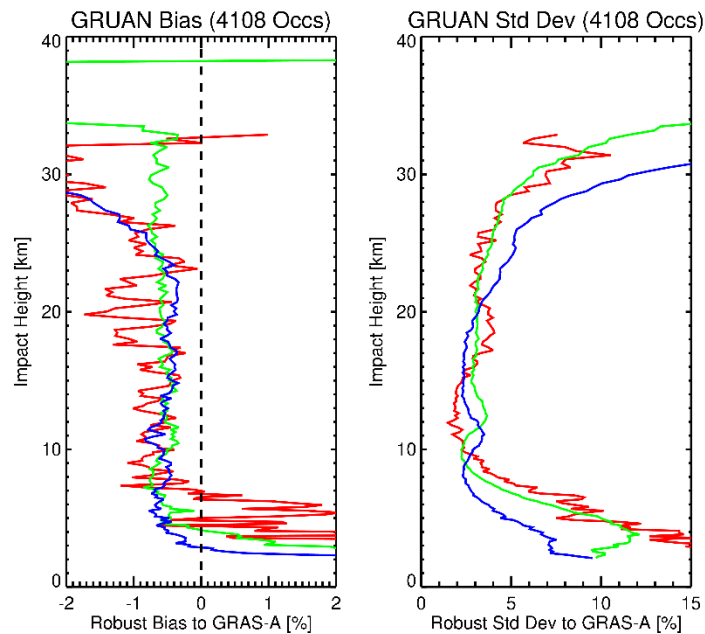
Bias and standard deviation of Lindenberg match against Metop-A (left), Lindenberg with reduced “AWI” like accuracy against Metop-A (right).
Legend provides coverage, average sondes/day, RO/match failures, outliers/weight.



Comparing to GRUAN v2 to GRAS Metop-A

www.eumetsat.int

Collocate Metop-A/GRAS 300km/3h against most GRUAN v2 sondes



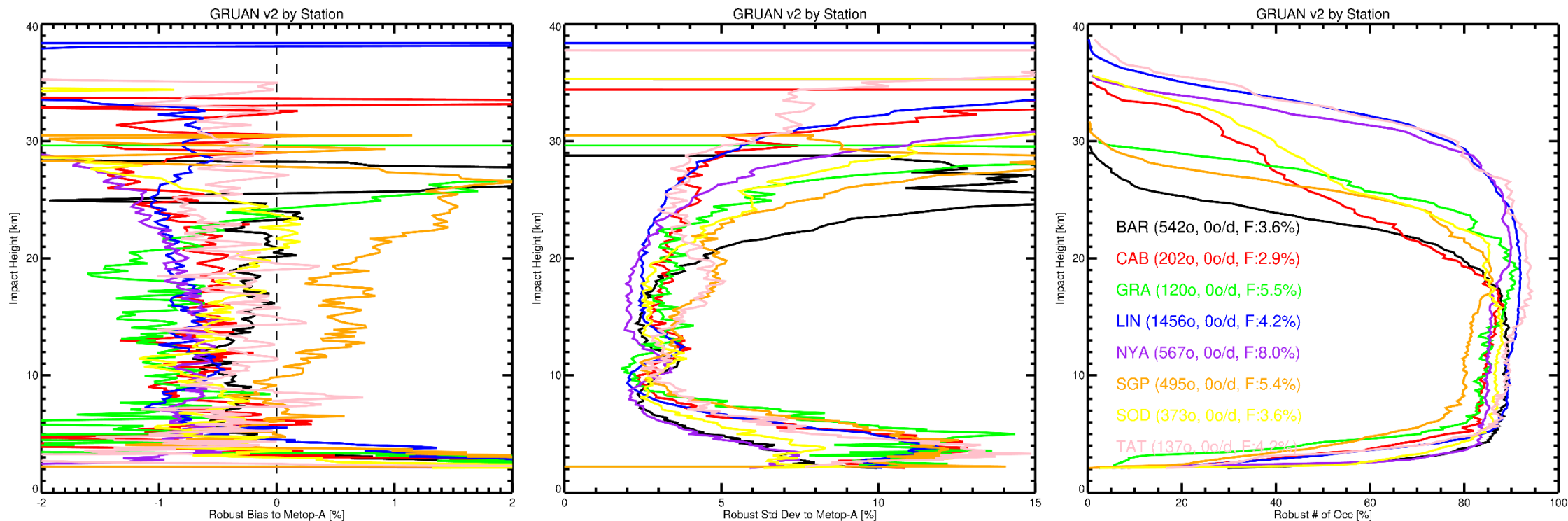
Bias and standard deviation of most GRUAN v2 matched against Metop-A (left), and against ECMWF ERA5 (right). Legend provides coverage, average sondes/day, RO/match failures, outliers/weight.



Comparing to GRUAN v2 by Station to GRAS Metop-A

www.eumetsat.int

Collocate Metop-A/GRAS 300km/3h against most GRUAN v2 sondes by station



Bias (left), standard deviation (middle), data availability (right) of several GRUAN v2 stations, matched against Metop-A. Legend provides total collocations, average sondes/day, RO/match failures.

Conclusion:

- Forward propagation radio sonde data to bending angles, for validation against each other, is possible with small bias (almost bias free below 25km)
- Could be useful for validation of bending angles in lower troposphere, as need for a priori use in RO processing is removed
- Current AWI Polarstern sonde data accuracy is insufficient to assess against radio occultation
- GRUAN v2 shows promising results

Future Work:

- Understand negative offset between sonde and GRAS (would correspond to about +30m height offset in GRUAN)
- Correct for collocation error
- Improve extrapolation of sonde profiles, using more robust upper refractivity gradient



Thank you!
Questions are welcome.